Energy transfers between Eu^{2+} and Er^{3+} in $EuGa_2S_4$:Er^{3+}

2004 J. Phys.: Condens. Matter 16 8075

(http://iopscience.iop.org/0953-8984/16/45/029)

INSTITUTE OF PHYSICS PUBLISHING JOURNAL OF PHYSICS: CONDENSED MATTER

J. Phys.: Condens. Matter **16** (2004) 8075–8084 PII: S0953-8984(04)82182-9

Energy transfers between Eu^{2+} and Er^{3+} in $EuGa_2S_4$:Er^{3+}

Charles Barthou[1], Paul Benalloul[1], Bahadur B Tagiev[2], Oktay G Tagiev[2], Said Abushov[2], Fatima A Kazimova[2] and Anatoly N Georgobiani[3]

[1] Laboratoire d'Optique des Solides, CNRS-UMR 7601, Université P&M Curie, 75252 Paris Cedex 05, France
[2] Institute of Physics of Azerbaijan, Academy of Sciences, Baku 370143, Azerbaijan
[3] P N Lebedev Physical Institute, Leninsky prospect 53, 119991 Moscow, Russia

E-mail: cbp@los.jussieu.fr (Charles Barthou)

Received 17 June 2004, in final form 30 July 2004
Published 29 October 2004
Online at stacks.iop.org/JPhysCM/16/8075
doi:10.1088/0953-8984/16/45/029

Abstract

The photoluminescence properties of $EuGa_2S_4$:Er polycrystals under 337.1 and 976 nm laser excitations versus temperature (78–500 K) are presented. Under 337.1 nm excitation wavelength, a wide emission band corresponding to Eu^{2+} ions in the visible range and emission lines of Er^{3+} in the visible and near infrared were observed. These emissions were also observed under 976 nm excitation wavelength with a two-photon absorption accompanied by a phonon assisted energy transfer to Eu^{2+} ions. According to experimental conditions, energy transfers from Eu^{2+} to Er^{3+} and from Er^{3+} to Eu^{2+} are highlighted.

1. Introduction

Erbium-doped materials are of great interest in thin film integrated photoelectronic technology due to their Er^{3+} intra-4f infrared (IR) emission at 1550 nm, a standard telecommunication wavelength in band C (1530–1560 nm). Dielectric thin films of different Er-doped materials can be used to fabricate planar optical amplifiers or lasers that can be integrated with communication systems. These questions have been reviewed recently by Poelman [1]. In wide bandgap materials, Er^{3+} ions also provide several emissions in the visible range.

It is well-known that the oscillator strengths of the Er^{3+} transitions are relatively weak and present narrow emission lines. An energy transfer mechanism from sensitizer to activator ions would allow one to obtain a more efficient phosphor. Energy transfers from Eu^{2+} as the sensitizer ions to Tb, Er, and Ho trivalent rare earth ions have already been reported, the mechanism being electric dipole–dipole interaction and phonon-assisted [2, 3] and three-step sensitization mechanisms based on the photoionization of Eu^{2+} ions [4]. The interest in that kind of energy transfer is due to the fact that Eu^{2+} has a strong broad absorption band, suitable

for optical pumping, while Ln^{3+} has sharp emission lines with much longer lifetimes, efficient for generating stimulated emission.

To our knowledge, luminescence processes have not been investigated for Eu^{2+}–Er^{3+} co-doping, either in the IR emission range or under near IR excitation (in the Er^{3+} excitation band around 980 nm). For this IR excitation the two-photon absorption can convert a near IR signal into an emission in the visible one and can be mainly explained by two mechanisms: the absorption of two photons takes place in only one Er^{3+} ion or this absorption takes place into two close neighbouring Er^{3+} ions followed by a cross-relaxation mechanism between these two ions [5–7]. The ratio between the visible and IR emission intensities will depend on the host material type and erbium concentration.

In some host matrices, due to the strong crystal field splitting of the ^{5}d levels of Eu^{2+}, the excitation bands of Eu^{2+} can be resonant with the Er^{3+} emission lines. Thus one can also expect a 'back' energy transfer from Er^{3+} to Eu^{2+} if one excites the Er^{3+} ions in the near IR range and obtains an emission of the ion Eu^{2+} in the visible range. The efficiency of this process will depend on the spectral overlap for the two-ion system Eu^{2+}–Er^{3+}.

Recently we have reported on the IR luminescence of Er^{3+} in calcium thiogallate [8]. This material belongs to the well-known family of ternary compounds with the general formula $M^{II}M^{III}_2(VI)_4$ (M^{II} = Mg, Ca, Sr, Ba, Eu, Yb, Sm; M^{III} = Al, Ga, In; VI = S, Se, Te) [9–11]. These materials are efficient phosphors when they are doped with rare earth ions.

To favour the energy transfer by decreasing the distances between the sensitizer ions and the activator ions, the ternary compound $EuGa_2S_4$ appears to us as a suitable host matrix for the Eu^{2+}–Er^{3+} doping system. In addition, the concentration quenching of the Eu^{2+} emission in thiogallates is relatively weak, with a reduction of the order of only 50% in $EuGa_2S_4$ compared to the optimal concentration in Ca and Sr thiogallates at room temperature [11]. This compound has an orthorhombic structure with space group $Fddd$ and lattice parameters $a = 2.0727$ nm, $b = 2.0454$ nm, and $c = 1.2197$ nm [10]. Eu atoms are surrounded by eight S atoms, and Ga atoms are located in the centre of tetrahedrons formed by four S atoms. This material is stable towards hydrolysis and presents a high solubility for any other rare-earth doping element.

The main task of this paper is to analyse the luminescence properties of Er^{3+} and Eu^{2+} in the IR and visible ranges under different excitation wavelengths and temperatures, the energy transfer between these two rare earth ions, and the up-conversion mechanism.

2. Sample and measurement details

$EuGa_2S_4$ undoped and Er^{3+} doped polycrystal samples were prepared by solid-phase synthesis from stoichiometric amounts of europium (EuS) and gallium (Ga_2S_3) sulfide powders in a sulfur vapour atmosphere at 1200 K followed by 1 h annealing treatment at 1000 K. Activation by Er (1, 5, and 7 at.% concentrations) was realized using ErF_3 doping during the synthesis process.

The photonic excitation at 337.1 nm or 420 nm was obtained by using respectively a pulsed nitrogen laser (Laser Photonics LN 1000, 1.4 mJ energy per pulse, pulse width 0.6 ns) or a dye laser (Laser Photonics LN102, Coumarine 420). For excitation at 976 nm, a continuous/pulsed laser diode was used up to 80 mW/600 mW power intensity. The emitted light from the sample, collected by an optical fibre located at 10 mm perpendicular to the surface, was analysed with a Jobin–Yvon spectrometer HR460 and a multichannel CCD Spectramax detector for the visible and near IR range, and with a TRIAX 320 and a multichannel PDA Hamamatsu detector for the IR range. The decays were analysed by a PM Hamamatsu R928 for the visible range and an InGaAs detector for the IR range, both coupled with a Nicolet 400 scope with a time constant of the order of 10 ns and 50 μs, respectively. The spectra were corrected in energy.

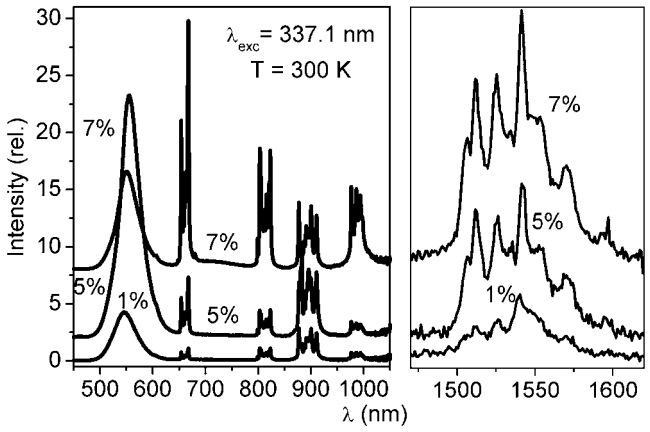

Figure 1. Luminescence spectra of $EuGa_2S_4$:Er^{3+} (Er = 1, 5, and 7 at.%) at room temperature under 337.1 nm excitation wavelength.

The experiments were carried out in a JanisVPF-600 Dewar with a variable temperature controlled between 78 and 500 K. The power intensity of the laser diode in the continuous state was limited at 80 mW in order to avoid heating of the sample by IR irradiation.

3. Results

3.1. Emission spectra under 337.1 nm UV excitation

The luminescence spectra of $EuGa_2S_4$:Er^{3+} phosphor for different Er^{3+} concentrations (1, 5, and 7 at.%) under nitrogen laser excitation (λ_{exc} = 337.1 nm) at room temperature are presented in figure 1. The first part of the spectra consists of a broad band assigned to the $4f^6 5d^1 \rightarrow 4f^7$ transition in Eu^{2+} ions with a maximum at 546, 555, and 550 nm for respectively 1, 5, and 7 at.%, in agreement with references [11] and [12]. The second part of the spectra consists of groups of lines at the intervals 650–675, 800–830, 870–920, 970–1000, and 1500–1600 nm, corresponding respectively to the $^4F_{9/2} \rightarrow {}^4I_{15/2}$, ($^4I_{9/2} \rightarrow {}^4I_{15/2} - {}^4H_{9/2} \rightarrow {}^4I_{9/2}$), ($^4G_{11/2} \rightarrow {}^4F_{9/2} - {}^4S_{3/2} \rightarrow {}^4I_{13/2}$), $^4I_{11/2} \rightarrow {}^4I_{15/2}$, and $^4I_{13/2} \rightarrow {}^4I_{15/2}$ transitions of Er^{3+} ions.

The intensity of the Eu^{2+} emission band versus the Er^{3+} concentration presents a maximum for 5 at.% Er^{3+} concentration. The intensity of the Er^{3+} transitions increases with Er^{3+} concentration except for ($^4G_{11/2} \rightarrow {}^4F_{9/2} - {}^4S_{3/2} \rightarrow {}^4I_{13/2}$) transitions (870–920 nm), which also present a maximum for 5 at.% of Er^{3+}. For this excitation wavelength and at room temperature, the Er^{3+} emissions at wavelengths shorter than 650 nm like transitions $^4S_{3/2} \rightarrow {}^4I_{15/2}$ (≈550 nm), $^2H_{11/2} \rightarrow {}^4I_{15/2}$ (≈530 nm) $^4F_{5/2} \rightarrow {}^4I_{15/2}$ (≈460 nm) and $^2H_{9/2} \rightarrow {}^4I_{15/2}$ (≈410 nm) were not observed, whereas they were already observed for $CaGa_2S_4$:Er [8] and $SrGa_2S_4$:Er [13]. Either these emissions are very low in intensity or the energy related to these excited levels is transferred to the Eu^{2+} ions. As we are interested in analysing the interaction between Eu^{2+} and Er^{3+}, the next results will be presented for the $EuGa_2S_4$ sample doped with 7 at.% Er^{3+} ions.

3.2. Excitation and emission spectra in the visible range

The excitation spectra for the emission of Eu^{2+} at 550 nm in $EuGa_2S_4$ and $EuGa_2S_4$:Er^{3+} (7 at.%) are very similar, with a broad band between 250 and 520 nm and a maximum at 485 nm (see figures 2 and 3) but they present some differences compared to the results given in [11] and [12]. In the $EuGa_2S_4$ compound the Eu^{2+} ions are surrounded by eight S^{2-} anions and occupy three different sites of symmetries, two D_2 and one C_2. However, in a first

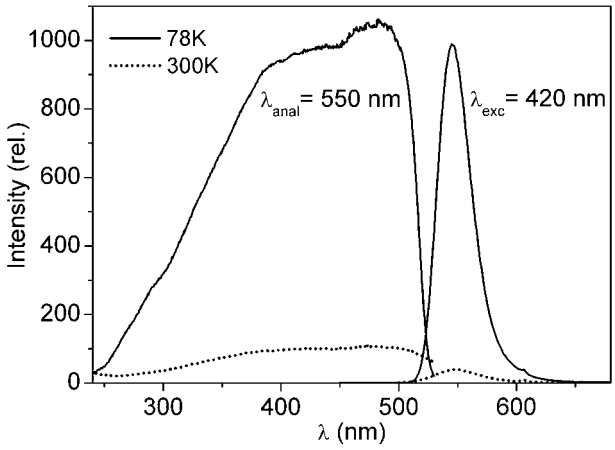

Figure 2. Emission and excitation spectra for $EuGa_2S_4$ under 420 nm excitation wavelength and 550 nm analysis wavelength respectively. T = 78 and 300 K.

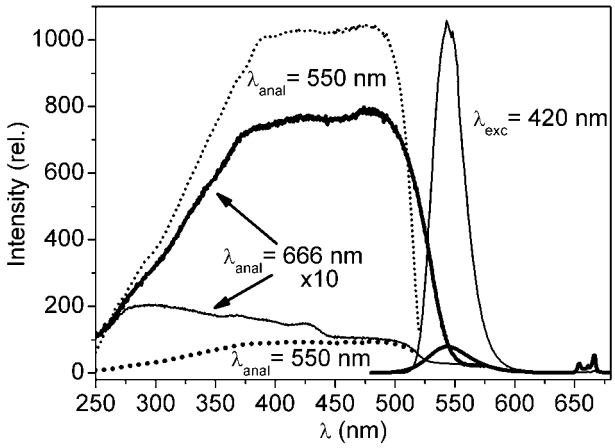

Figure 3. Emission and excitation spectra for $EuGa_2S_4$:Er^{3+} (7 at.%) under 420 nm excitation wavelength and 550 and 666 nm analysis wavelength respectively. Fine curves: T = 78 K, thick curves T = 300 K.

approximation we can consider that the S^{2-} anions form an almost square based anti-prism, in the centre of which the Eu^{2+} ion is placed. If we consider this higher symmetry D_{4D}, the 5d orbitals are split into three levels, in order of increasing energy a_1 (orbital dz^2), e_2 (orbitals dx^2–y^2 and dxy) and e_3 (orbitals dxz and dyz). In the case of $SrGa_2S_4$:Eu^{2+}, only the two transitions of lower energy are observed, the higher third level being in the conduction band of $SrGa_2S_4$ [9, 14]. For $EuGa_2S_4$, it is not possible to separate these two lower excitation bands, even at low temperature. The charge transfer band associated to an electron transfer from the highest filled molecular orbital to the partly filled 4f shell of the Er^{3+} ions [15] is also masked by the excitation bands of the Eu^{2+} ions.

Figures 2 and 3 present, for two temperatures (78 and 300 K) the emission spectra respectively for $EuGa_2S_4$ and $EuGa_2S_4$:Er (7 at.%) for a direct excitation of the Eu^{2+} ions (420 nm). For the $EuGa_2S_4$ ($EuGa_2S_4$:Er (7 at.%)) sample, with an increase of temperature from 78 to 500 K, the Eu^{2+} luminescence band presents a peak shift from 545 to 554 nm (543–548 nm) and an increase of FWHM from 34 to 60 nm (30–59 nm). At the same time, the temperature quenching is of the order of 20 (10) at 300 K and 200 (100) at 500 K compared to 78 K (see figure 4). The temperature quenching for $EuGa_2S_4$ is of the same order as previously reported [11, 12].

Under this excitation wavelength (420 nm) we also observe some Er^{3+} ion emissions at 666 nm due to the $^4F_{9/2} \rightarrow {}^4I_{15/2}$ transitions, as well as very weak emissions at 550 nm due to

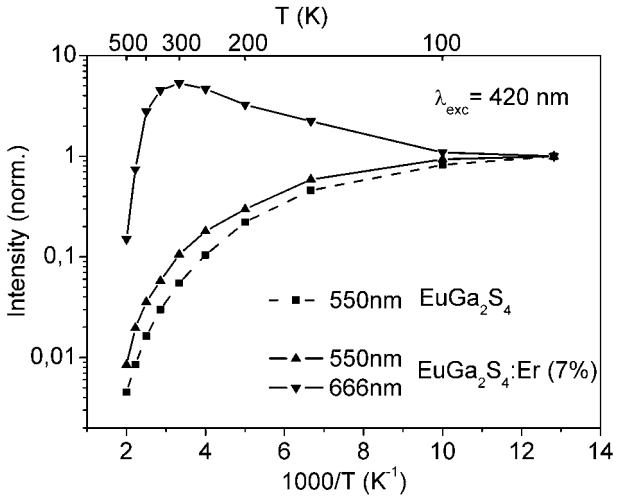

Figure 4. Luminescence temperature quenching of Eu^{2+} and Er^{3+} emissions for $EuGa_2S_4$ and $EuGa_2S_4$:Er (7 at.%) under 420 nm excitation wavelength.

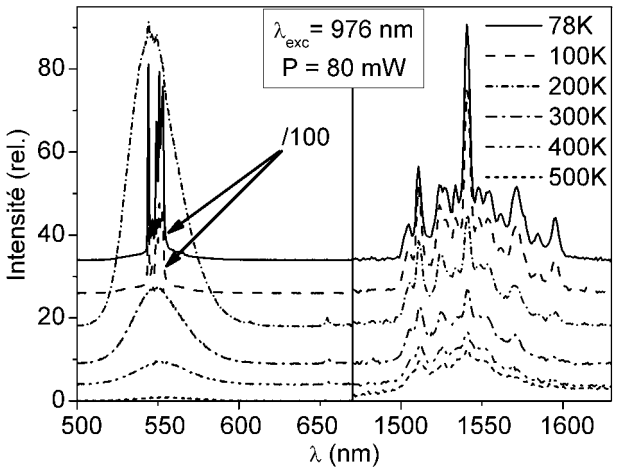

Figure 5. Luminescence spectra of $EuGa_2S_4$:Er^{3+} (7 at.%) under 976 nm excitation wavelength at different temperatures.

the $^4S_{3/2} \rightarrow {}^4I_{15/2}$ transitions. The emissions at 550 nm are only observed at low temperature, and they disappear when the temperature increases above 150 K. While the emission of Eu^{2+} decreases according to temperature, we also note for this 420 nm excitation that the Er^{3+} emission intensity at 666 nm increases until 300 K and is quenched above this temperature (see figure 4). The other Er^{3+} emission lines in the visible range already observed under 337.1 excitation wavelength were not detected for this 420 nm excitation wavelength.

The excitation spectrum for the Er^{3+} emission recorded at 666 nm wavelength, for which Eu^{2+} emission is not at all present, exhibits a different thermal dependence compared to the excitation spectrum for the Eu^{2+} emission (see figure 3). At low temperature the maximum of the excitation band peaks at 300 nm. When the temperature increases, the intensity of this band at 300 nm remains almost the same when the typical excitation band of Eu^{2+} increases.

3.3. Emission spectra under near-IR excitation (976 nm)

The luminescence spectra of $EuGa_2S_4$:Er versus temperature under continuous diode laser excitation at $\lambda_{exc} = 976$ nm in the $^4I_{11/2}$ Er^{3+} levels with a power of 80 mW are presented in figure 5.

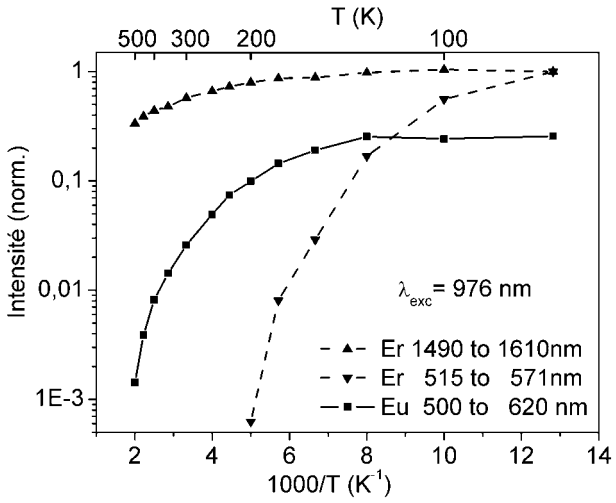

Figure 6. Luminescence temperature quenching of Eu^{2+} and Er^{3+} emissions for $EuGa_2S_4$:Er (7 at.%) under 976 nm excitation wavelength.

At 78 K, we observe mainly the Er^{3+} emission corresponding to the $^4S_{3/2} \rightarrow {}^4I_{15/2}$ transitions at 550 nm and a relatively lower Eu^{2+} emission. As in the case of $\lambda_{exc} = 420$ nm, the $^4S_{3/2} \rightarrow {}^4I_{15/2}$ emission disappears for temperatures higher than 200 K. Very weak Er^{3+} emissions corresponding to the $^2H_{11/2} \rightarrow {}^4I_{15/2}$ transitions at 530 nm and to the $^4F_{9/2} \rightarrow {}^4I_{15/2}$ transitions at 660 nm were also observed. A relatively intense IR luminescence at 1530 nm is observed due to $^4I_{13/2} \rightarrow {}^4I_{15/2}$ transitions.

In figure 6 the temperature quenching of the different Er^{3+} emissions compared to the Eu^{2+} emission is presented. The emitted energy for the two Er^{3+} emissions is normalized to the value obtained at $T = 78$ K. The emitted energies for the Er^{3+} emission (515–571 nm) and the Eu^{2+} emission are given in relative values.

When the temperature increases, the intensity of Eu^{2+} emission remains constant up to 125 K and presents a quenching for higher temperatures. This was not the case under 420 nm excitation wavelength, for which the temperature quenching appears as soon as the temperature increases above 78 K (see figure 4). The two main emissions of Er^{3+} ions ($^4S_{3/2} \rightarrow {}^4I_{15/2}$ and $^4I_{13/2} \rightarrow {}^4I_{15/2}$) do not have the same temperature quenching. While the emission at 550 nm disappears above 200 K, the emission at 1530 nm presents only a quenching of a factor 1.5 at 300 K and 3 at 500 K.

3.4. Decay curves

To analyse the influence of the Er doping on the decay curves of the Eu^{2+} emissions, it is necessary first to look at the decays for non-doped $EuGa_2S_4$.

For a direct excitation of Eu^{2+} at 420 nm, the decay curves recorded at 543 nm do not present any exponential part (see figure 7). The decays are faster when the temperature is higher, the τ_e value decreasing from 205 ns to 55 ns and 33 ns respectively for T being 77, 300, and 400 K. Donohue *et al* have reported a value of 0.16 μs for this decay at room temperature.

These Eu^{2+} decays in the $EuGa_2S_4$ host matrix are very different compared with the decays of Eu^{2+} in other thiogallates like $CaGa_2S_4$ and $SrGa_2S_4$, for which the decays are exponential at 77 K with a τ value of 480 ns [16, 17].

The decays of the Eu^{2+} emission for the Er doped sample (7 at.%) at 420 nm excitation wavelength are always longer than for the pure $EuGa_2S_4$ sample for the same temperature (see figure 8), in agreement with the relative intensity of the total photoluminescence versus

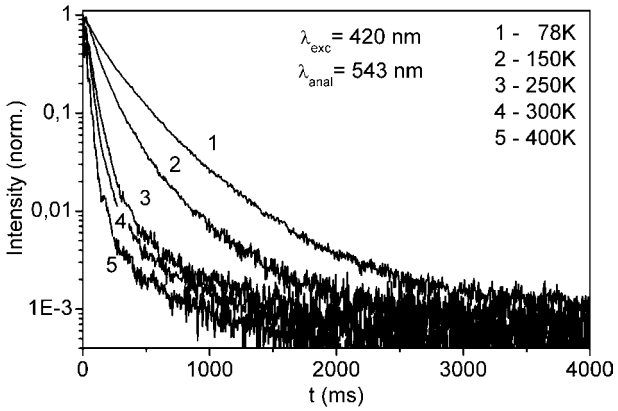

Figure 7. Luminescence decays of 543 nm Eu^{2+} emission in $EuGa_2S_4$ under 420 nm excitation wavelength versus temperature.

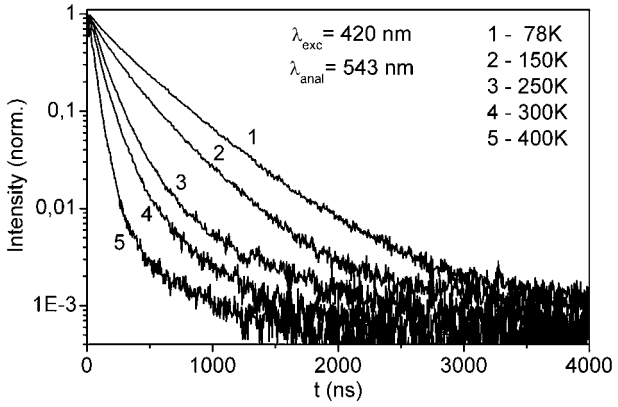

Figure 8. Luminescence decays of 543 nm Eu^{2+} emission in $EuGa_2S_4$:Er^{3+} (7 at.%) under 420 nm excitation wavelength versus temperature.

temperature for these two kinds of samples which are presented in figure 4. At 78 K the Eu^{2+} decay presents an exponential part over two decades, with a decay time of the order of 400 ns. For higher temperatures the decays are faster, not exponential and τ_e decreases from 340 ns at 78 K to 97 ns at 300 K and 61 ns at 400 K. For temperatures below 100 K, the decay curves are the same for the three different Er concentrations. For higher temperatures the decay for the 7 at.% sample is a little faster.

The decay curve for the $^4I_{13/2} \rightarrow {}^4I_{15/2}$ transition of Er^{3+} ($\lambda_{exc} = 972$ nm, $\lambda_{anal} = 1530$ nm) recorded at room temperature is shown in figure 9. The first part of this curve presents a rise time connected with the population of the $^4I_{13/2}$ level through the de-excitation process $^4I_{11/2} \rightarrow {}^4I_{13/2}$. The decay part can be fitted with an exponential function with a life time $\tau \approx 3$ ms.

4. Discussion

4.1. $EuGa_2S_4$ host matrix properties

The luminescence data concerning the $EuGa_2S_4$ host matrix allow us to determine several parameters helpful in describing the radiative properties of this phosphor.

Using a single configuration coordinate model, the intensity of the vibronic transitions is proportional to the $e^{-S}S^n/n!$ factor, where S is the Huang–Rhys parameter and it measures the interaction between the luminescent centre and the vibrating lattice [18]. With a zero

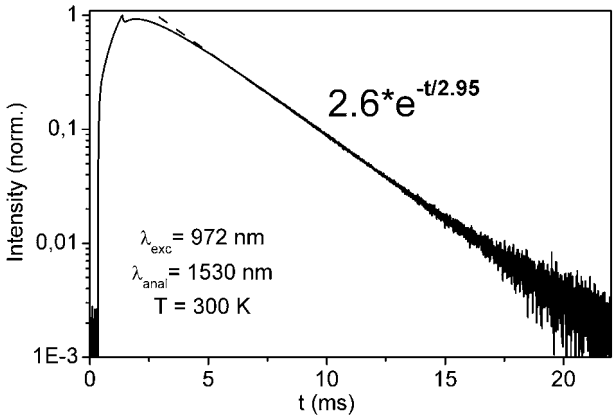

Figure 9. Luminescence decay of 1530 nm Er^{3+} emission in $EuGa_2S_4$:Er^{3+} (7 at.%) under 972 nm excitation wavelength. $T = 300$ K.

phonon line evaluated at 2.37 eV, the best fit for the Eu^{2+} emission band at 77 K is for $S = 3.3$ and $h\nu = 33$ meV. With these data, the Stokes shift is $(2S - 1)h\nu = 0.22$ eV. We used the following equation to fit versus the temperature the variation of FWHM for the Eu^{2+} emission band [19]:

$$\Gamma(T) = \sqrt{8 \ln 2} x h\nu x \sqrt{S} x \sqrt{\coth\left(\frac{h\nu}{2kT}\right)}.$$

The best fit was obtained with the same value already found, i.e. $S = 3.3$ and $h\nu = 33$ meV. The value of the lattice phonon energy is in agreement with the most intense Raman vibration energy found for the $EuGa_2S_4$ compound [20].

The non-exponential decay curves of the Eu^{2+} emission and their behaviour versus temperature indicate a strong concentration quenching related to an energy diffusion process which can be assisted by phonons and with the intervention of traps. In such a compound the distance between Eu ions is of the order of 0.55 nm. The decays being strongly non-exponential, it is not possible to characterize the thermal quenching with an activation energy related to $1/\tau_{nr}$ through the function $1/\tau(T) = 1/\tau_0 + 1/\tau_{nr}(T)$ [21].

In spite of this strong concentration quenching, the efficiency at 300 K of the $EuGa_2S_4$ phosphor is only half the intensity of Eu^{2+}-doped Ca or Sr thiogallates for which the optimal content is of the order of 2–4 mol% [11]. But at 78 K when the two later phosphors present quite the same luminescence intensity, $EuGa_2S_4$ provides a photoluminescence increased by a factor 20. One can conclude that this $EuGa_2S_4$ is a very efficient phosphor for the emission of Eu^{2+} at 550 nm, but only at low temperature.

4.2. Energy transfer processes

The energy transfer from Eu^{2+} to Er^{3+} for an excitation at 420 nm cannot be deduced from the influence of the Er doping on the decay curves of the Eu^{2+} emissions. Such Er doping may limit the energy diffusion process between Eu^{2+} ions and therefore may provide longer decays. On the other hand, $Eu^{2+} \rightarrow Er^{3+}$ energy transfer may provide faster decays. Our results presented in figure 8, that the decays are longer due to the Er doping, can be explained by considering the first process more efficient than the second one.

Our results indicate that energy transfer mechanisms from Er^{3+} to Eu^{2+} and from Eu^{2+} to Er^{3+} influence the emission properties of these samples. These two mechanisms are in competition, and the dominating one will depend on the sample temperature.

If one analyses the excitation spectra, the maximum energy of the excitation band at 300 nm for the Er^{3+} emission at 660 nm in $EuGa_2S_4$:Er (7 at.%) ($\leqslant$150 K) corresponds to the

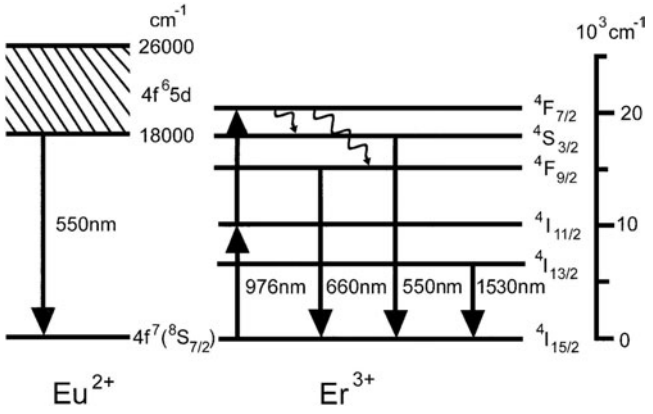

Figure 10. Scheme of the up-conversion process and $Er^{3+} \rightarrow Eu^{2+}$ energy transfer process in $EuGa_2S_4$:Er^{3+} (7 at.%) under 976 nm excitation wavelength.

wavelength of the $^4I_{15/2} \rightarrow {}^2K_{13/2}$ transitions of the Er^{3+} ion. But no fine structure with narrow lines was observed. As this band does not correspond to a direct Eu^{2+} excitation band, this 300 nm band corresponds to the fundamental absorption of $EuGa_2S_4$. The band gap energy, estimated at 4.1 eV, can be compared to 4.4 eV obtained for Ca [22] and Sr [14] thiogallates. For this reason we suppose that excitation of Er^{3+} ions corresponds to an energy transfer from the $EuGa_2S_4$ lattice in this temperature range. This absorption band is very close to the direct excitation band of the Eu^{2+} ions, and this is the reason why this band is not clearly observed in the excitation spectra of Eu^{2+} emission.

Under an excitation in the near UV (337.1 nm) which allows the excitation of Er^{3+} ions and Eu^{2+} ions, we observe, in addition to the emission of Eu^{2+}, only the emissions of Er^{3+} longer in wavelength than the Eu^{2+} emission band. This confirms an energy transfer from Er^{3+} ions to Eu^{2+} ions.

If we analyse the emissions under a direct excitation of the Eu^{2+} ions at 420 nm, without a direct excitation of the Er^{3+} ions, we observe in addition to the emission band of Eu^{2+} ions the emission lines of Er^{3+} ions at lower energy. Thus we are in the presence of a $Eu^{2+} \rightarrow Er^{3+}$ energy transfer, a transfer which is confirmed by the excitation spectra for the Er^{3+} emissions.

Looking at the behaviour of these samples under excitation in the near IR (976 nm), we have a mechanism of up-conversion inside the levels of the Er^{3+} ions, but in addition to the Er^{3+} emissions, we observe the emission of Eu^{2+} ions.

Concerning the up-conversion mechanism, two principal processes can be considered to allow the excitation of the $^4F_{7/2}$ level of Er^{3+} ions under a 976 nm excitation. Either two photons are absorbed by only one ion ($^4I_{15/2} \rightarrow {}^4I_{11/2} \rightarrow {}^4F_{7/2}$), or two excited close Er^{3+} ions can interact to give only one excited Er^{3+} ion with higher energy. The first mechanism depends only on the laser power, while the second also depends on the Er^{3+} concentration. Unfortunately we observed a heating of the sample when the power was higher than 80 mW, and we could not obtain useable results versus the excitation laser power to determine which of these two mechanisms is more efficient in this sample.

Moreover, the relative intensities of the emissions of the Er^{3+} ions and Eu^{2+} ions depend on the sample temperature. We are in the presence of a competition process between $Er^{3+} \rightarrow Eu^{2+}$ and $Eu^{2+} \rightarrow Er^{3+}$ energy transfers. When the temperature increases, the excitation band of Eu^{2+} shifts to the red wavelength (see figure 3) and can superpose to the $^4S_{3/2}$ levels of Er^{3+}. An energy transition scheme is presented in figure 10. These $^4S_{3/2}$ levels of Er^{3+} are very close to the first excited level $4f^65d$ for Eu^{2+}. Then the resonance transition from the $^4S_{3/2}$ level of Er^{3+} to the $4f^65d$ level of Eu^{2+} takes place, but it depends on the temperature.

At low temperature, the $Eu^{2+} \rightarrow Er^{3+}$ transfer is more important, while at higher temperature the two transfers are possible. As the oscillator strength of the transition for Eu^{2+} ions is more important than for Er^{3+}, the emission of Eu^{2+} will dominate when the temperature increases.

5. Conclusion

We have shown that in europium thiogallate doped with Er^{3+} ions, the strong concentration of Eu^{2+} allows a very strong interaction with the Er^{3+} ions. An energy transfer mechanism occurs from Eu^{2+} ions to Er^{3+} ions, but the inverse mechanism was also observed. A phenomenon of up-conversion was highlighted with traditional emissions of the Er^{3+} ions but also, with the energy transfer mechanism, the emission of the Eu^{2+} band in this ternary compound. Thus it is possible to obtain a very intense green emission at 545 nm under excitation in the near IR. For an excitation in the 300–550 nm range, the emission in the IR corresponding to one of the windows of optical fibres containing silica (band C at 1530 nm) is enhanced by this very effective $Eu^{2+} \rightarrow Er^{3+}$ energy transfer process.

Acknowledgments

This work was supported by a collaborative linkage grant No 979350 from NATO, an RFBR—NSFCC grant No 02-02-39007, and CNRS/Academy of Sciences of Azerbaijan project No 16994.

References

[1] Poelman A 1997 *J. Appl. Phys.* **82** 1
[2] Xingren L, Gang X and Powell R C 1986 *J. Solid State Chem.* **62** 83
[3] Latourrette B, Guillen F and Fouassier C 1979 *Mater. Res. Bull.* **14** 865
[4] Jouart J P, Bissieux C, Mary G and Egée M 1985 *Phys. Status Solidi* b **132** 619
[5] van den Hoven G N, Snoeks E, Polman A, van Dam C, van Uffelen J W M and Smit M K 1996 *J. Appl. Phys.* **79** 1258
[6] Chukova Yu P 1980 *AntiStokes Luminescence and New Application Possibilities* (Moscow: Soviet Radio) p 192
[7] Johnson L F, Guggehheim H J, Rich T C and Ostermayer F W 1972 *J. Appl. Phys.* **43** 1125
[8] Georgobiani A N, Gruzintsev A N, Barthou C, Benalloul P, Benoit J, Tagiev B G, Tagiev O B and Dzhabbarov R B 2001 *J. Electrochem. Soc.* **148** H167
[9] Peters T E and Baglio I A 1972 *J. Electrochem. Soc. Solid State Sci. Technol.* **119** 230
[10] Roques R, Rimet R, Declereq J P and Germain G 1979 *Acta Crystallogr.* B **35** 555
[11] Donohue P C and Hanlon J E 1974 *J. Electrochem. Soc. Solid State Sci. Technol.* **121** 137
[12] Iida S, Kato A, Tanaka M, Najafov H and Ikuno H 2003 *J. Phys. Chem. Solids* **64** 1815
[13] Garcia A, Fouassier C and Dougier P 1982 *J. Electrochem. Soc.* **129** 2063
[14] Chartier C, Barthou C, Benalloul P and Frigerio J-M 2004 *J. Lumin.* at press
[15] Garcia A, Ibanez R, Fouassier C and Hagenmuller P 1984 *J. Lumin.* **26** 389
[16] Benalloul P, Barthou C, Fouassier C, Georgobiani A N, Lepnev L S, Emirov Y N, Gruzintsev A N, Tagiev B G, Tagiev O B and Jabbarov R B 2003 *J. Electrochem. Soc.* **150** G62
[17] Eichenauer L, Jarofke B, Mertins H-C, Dreyhsig J, Busse W, Gumlich H-E, Benalloul P, Barthou C, Benoit J, Fouassier C and Garcia A 1996 *Phys. Status Solidi* a **153** 515
[18] Shionoya S and Yen W M 1998 *Phosphors Handbook* (Boca Raton, FL: CRC press) chapter 2
[19] Henderson B and Imbush G F 1989 *Optical Spectroscopy of Inorganic Solids* (Oxford: Clarendon)
[20] Chartier C, Jabbarov R, Jouanne M, Morhange J-F, Benalloul P, Barthou C, Frigerio J-M, Tagiev B and Gambarov E 2002 *J. Phys.: Condens. Matter* **14** 3693
[21] Curie D 1963 *Luminescence in Crystals* (London: Methuen)
[22] Hidaka C and Takizawa T 2002 *J. Cryst. Growth* **237–239** 2009